Computer Fraud and Security
ISSN (online): 1873-7056

Modeling of PV Power Based on Weather Random Sampling and Fluctuation Characteristics Simulation

Zhenzhen Wang[1], Ruiqing Fan[1], Quanyou Li[1], Lingxu Guo[2], Jiaan Zhang[3,*]

[1]State Grid Tianjin Electric Power Company Wuqing Power Supply Branch, Tianjin 301700, China

[2]State Grid Tianjin Electric Power Company, Tianjin 300000, China

[3]School of Electrical Engineering, Hebei University of Technology, Tianjin 300401, China

**Corresponding Author.*

Abstract:

In response to the significant fluctuations in PV power generation due to weather changes, this paper proposes a time-series modeling approach. The proposed method integrates random weather sampling with fluctuation characteristic simulation techniques, effectively characterizing the uncertainty of PV power. Initially, the characteristics and the fluctuation of PV power under different weather conditions are analyzed, and the impact of weather factors on PV power fluctuations is quantified using the "no-shade coefficient". Subsequently, based on statistical analysis of historical weather data, a Markov chain-based weather type transition model is constructed to accurately capture the transition patterns between weather types. On this foundation, combined with the Gaussian Mixture Model (GMM) and the Normal Distribution, mean value and fluctuation value models of the PV power no-shade coefficient are established, respectively. These two models collectively provide a detailed depiction of PV power fluctuations. Finally, the validity and accuracy of the proposed modeling method are verified using actual operational data from a PV power station in Wuqing, Tianjin. This method provides a modeling basis and algorithmic support for the new electricity system planning and production process simulation.

Keywords: PV power, no-shade coefficient, random weather sampling, fluctuation modeling, Markov chai

INTRODUCTION

Driven by the Carbon Peaking and Carbon Neutrality Goals, China's traditional fossil energy-led power system is accelerating the transition to a new power system centered on new energy [1,2]. Photovoltaic power generation, as a kind of clean and renewable energy, plays a crucial role in the process of building a new power system. With the continuous progress of technology and cost reduction, photovoltaic power generation has gradually become the new favorite of the power market, especially in the distribution network, photovoltaic in the form of a large number of distributed power supply access, has become an important trend in the development of the current power system [3]. However, the output of PV power is highly susceptible to significant effects of weather conditions (e.g., light intensity and cloud cover) [4,5], resulting in significant volatility and unpredictability of PV power output, which constitutes a significant challenge to the smooth operation of the power grid. Therefore, quantitative analysis of PV fluctuation characteristics is crucial for operational analysis and PV prediction of high percentage new energy power systems [6].

Grasping the fluctuation characteristic of PV output is of great significance to the security, stability and economic operation of the power system [7]. At present, there are two main ways to quantify PV volatility [8]: the first way is to start from the overall shape of the waveform, firstly to clearly define the type of fluctuation, and then to extract the key characteristic quantities of fluctuation, and to explore them in depth through methods such as cluster analysis. The second approach is to start from the partial frequency waveform, and study the fluctuation characteristics of different frequency bands by decomposing the PV output power. Therefore, a combined time-varying filter empirical mode decomposition (TVF-EMD) and extreme learning machine (ELM) model constructed to handle the fluctuating characteristics of the PV power data is utilized, and the bias of the model prediction due to the volatility of the PV output is investigated to point out the impact of this bias on the microgrid frequency [9,10]. In addition, the uncertainty of PV output is modeled using change point detection, cyclic k-mean clustering (KMC), and Monte Carlo simulation (MCS), followed by the construction of a hybrid prediction model for deterministic and uncertainty prediction to study the impact of PV output on the dynamic currents. A new power system flexibility assessment model is proposed to analyze the fluctuation characteristics of PV output and study the impact of the fluctuation characteristics of PV output on the system [11-13]. Finally, a detailed and

comprehensive review of the factors affecting the efficiency of solar cells is carried out to address the low efficiency of PV power generation. A detailed review of the materials underlying the solar cells is presented [14].

Weather type variation is one of the main reasons for intermittent fluctuations in PV power generation. First, based on the severe weather dataset and the corresponding PV power output, the impact of extreme weather events on PV performance was analyzed, and the effect of temperature on PV power generation efficiency under different weather conditions was investigated [15].

The PV data were categorized according to weather type by a multidimensional clustering method, and the historical power data were decomposed by a decomposition model, and the improved model was used to predict the PV power under different weather conditions [16-17].

In addition, an extreme scenario generation method that can fully exploit the correlation between historical new energy data is proposed, which is based on the information maximization generative adversarial network (InfoGAN) to generate extreme scenarios throughout the year, and provides effective theories and methods for the safe operation of the new power system [18].

Existing studies have improved the accuracy of PV power prediction to some extent by quantifying PV fluctuations and classifying weather types. However, there are still deficiencies in combining the two and constructing uncertainty time-series models of PV output based on statistical features:

1) Further uncertainty quantification analysis is still needed for the fluctuation characteristics of photovoltaic output under various weather conditions;

2) For the evolution pattern of complex weather types, the intrinsic uncertainty mechanism needs to be further explored.

In view of this, this study proposes a modeling technique for PV output volatility. The specific research work includes:

1) The probability of occurrence of various types of weather and its changing law were statistically analyzed and modeled;

2) For different weather types, the volatility characteristics of PV output were analyzed with uncertainty, and its probabilistic statistical model was constructed;

3) Taking the operation data of a PV power station in Wuqing area of Tianjin as a case study, the modeling method is empirically tested.

TEMPORAL VOLATILITY CHARACTERISTICS OF PHOTOVOLTAIC OUTPUT

In order to simplify the analysis process and clarify the inherent uncertainty mechanism of PV output [19], the PV output is divided into deterministic and uncertainty components. Specifically, the PV output under ideal unshaded sunny day conditions is considered as the deterministic benchmark, i.e., the "no-shade output". The deviation of the actual PV output from this benchmark is regarded as the uncertainty component, which is quantified by calculating the ratio of the actual output to the no-shade output, which is defined as the "no-shade coefficient".

In the specific analysis, the no-shade output can be calculated using the peaks at each daily time point in a period of historical data, as shown in Equation (1).

$$w_j = \max\left(Pv_{1j}, Pv_{2j}, \cdots, Pv_{ij}, \cdots, Pv_{mj}\right) \tag{1}$$

In the equation, wj represents the PV output at the j-th moment under no-shade conditions; Pvij represents the PV output at the j-th moment of day i; m corresponds to the number of days of historical data, and max(.) is the function of taking the maximum value.

If the PV output at a certain moment j is P_{vj}, its corresponding no-shade coefficient u_j is calculated as shown in Equation (2).

$$u_j = \frac{Pv_j}{w_j}, u_j \in [0,1] \tag{2}$$

The no-shade coefficient reflects to a certain extent the influence of weather type, light intensity, etc. on the fluctuation of PV output, and the variation of the no-shade coefficient of PV output for a time period of 1 year is given in Figure 1. Figure 2 gives the curves of the no-shade coefficient for five weather types such as sunny, cloudy, overcast sky, hazy, rain and snow.

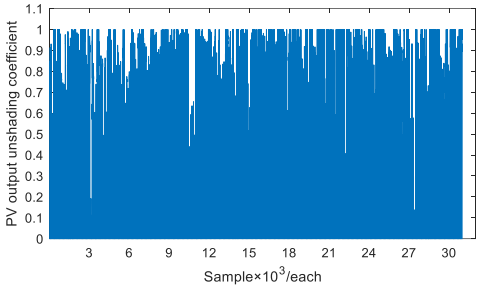

Figure 1. The annual variation of the no-shade coefficient of PV output

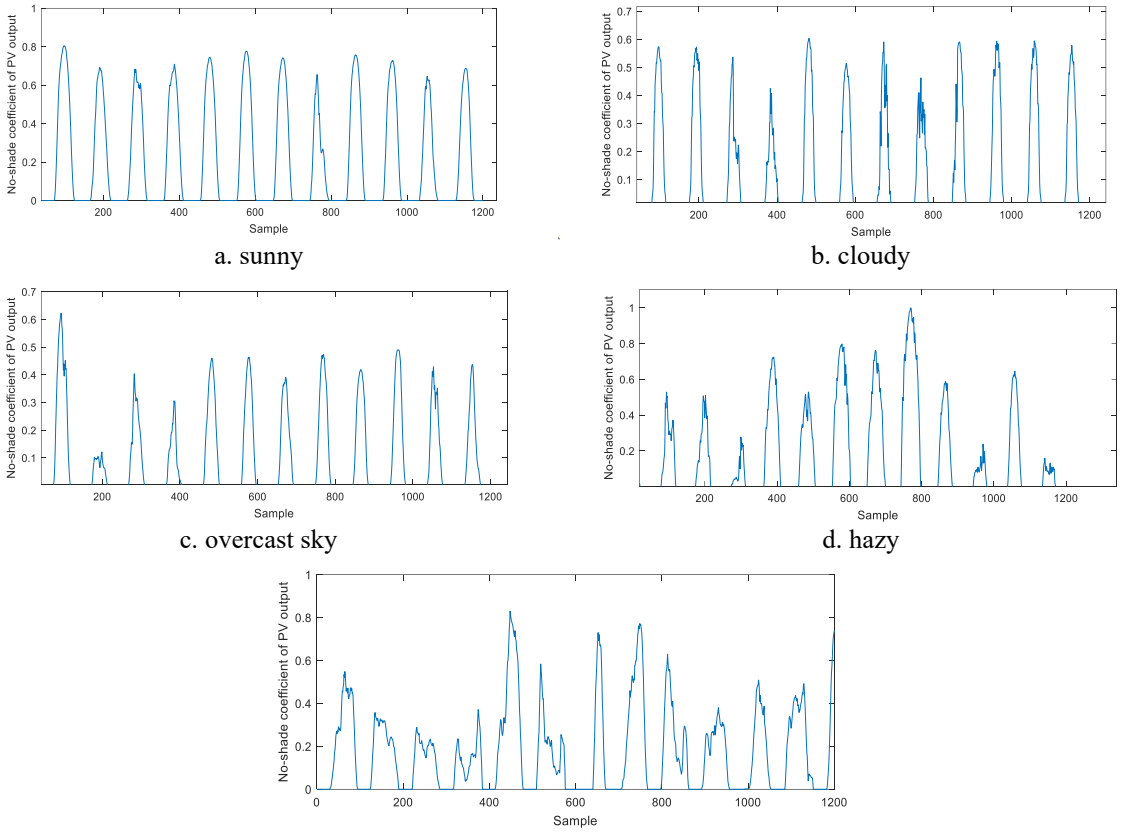

a. sunny

b. cloudy

c. overcast sky

d. hazy

e. rain and snow

Figure 2. The no-shade coefficient of PV output for 5 weather types

In general, the no-shade coefficient of a sunny day is higher with less fluctuation; The no-shade coefficient of a cloudy day fluctuates greatly, and the overall PV output level is lower than that of a sunny day; The no-shade coefficient of an overcast day is lower with less fluctuation; In a hazy weather, the particulate matter in the air scatters and absorbs the solar radiation, so that the PV output decreases, corresponding to the decrease in the no-shade coefficient, which can be regarded as an extreme case of an overcast day; The rain and snow day, with a thick layer of clouds and often accompanied with precipitation, the PV output is almost zero, corresponding to a very low or zero level of PV output. The PV output is almost zero, corresponding to a very low or zero no-shade

coefficient. The weather types in Figure 2 are classified in terms of days, but it should be noted that the weather types may change at different moments of the same day, which makes it more complicated to characterize the PV output for different weather types.

There are two ways to characterize the time-series volatility of PV output based on the no-shade coefficient, either by using the difference between the back-sequence value and the front-sequence value in the time series shown in Equation (3), or by using the difference between the value and the mean value at each moment in the time series shown in Equation (4).

$$\Delta u_1 = \left\{u_2 - u_1, u_3 - u_2, \cdots, u_n - u_{n-1}\right\} \tag{3}$$

$$\Delta u_2 = \left\{u_1 - \bar{u}, u_2 - \bar{u}, \cdots, u_n - \bar{u}\right\} \tag{4}$$

Considering that the PV output and its corresponding no-shade coefficient are greatly affected by weather factors and that the level of PV output under the same type of weather conditions may also differ greatly, the second way of characterizing the volatility of PV output shown in Equation (4) is chosen here. In this characterization method, the calculation of the volatility value requires the mean value information of the PV output, and its calculation can adopt the method of time window. The selection of the time window width is based on the time interval between the PV data and the meteorological data series, and if the time interval of the PV data is smaller than that of the meteorological data, the time interval of the meteorological data is mainly referred to determine the time window width. The maximum recommended time window width is 1 day, and if the data conditions allow, the time window width can be taken as 2 hours or 1 hour.

MODELING OF PV OUTPUT TIME-SERIES VOLATILITY

Weather Type Model

There may be differences in the division of the main types of weather in different regions, and in this paper, the main types of weather are divided into: sunny (S1), overcast sky (S2), cloudy (S3), hazy (S4), and rain and snow (S5) types. In practice, the change of weather type may be affected by a variety of factors, including seasons, geographic location, climate patterns, etc. Here, in terms of modeling the output volatility of photovoltaic power generation, it is assumed that: the current weather type is only related to the previous moment, and has nothing to do with the weather conditions before the previous moment, which can then be based on the Markov chain for modeling the change of weather type.

Based on the weather types set above, the state space of the Markov chain weather type change model is S={S1, S2, S3, S4, S5}, and there is mainly the uncertainty problem of transfer probability in the modeling process. State S4 corresponds to the generation of hazy weather is not completely natural, and its generation is the result of a combination of factors, including meteorological conditions, topography and pollutant emissions. In recent years, with the strengthening of environmental protection and the management of pollutant emission sources, the meteorological conditions for haze formation are gradually improving. From the statistical data in Figure 3, the years with more haze weather in Tianjin are from 2014 to 2020, and the number of occurrences in recent years is significantly reduced, which should be taken into account in the calculation of the transfer probability, corresponding to the treatment of the data in recent years is prioritized to meet the premise of convergence to be calculated.

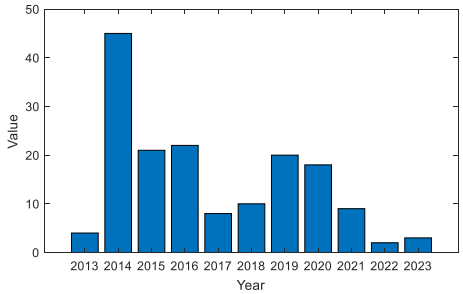

Figure 3. Statistics on the occurrence of haze weather in Tianjin

Table 1. State transition matrix for weather changes in Tianjin over the past 3 years

State	S1	S2	S3	S4	S5
S1	0.496	0.336	0.122	0.016	0.03
S2	0.322	0.416	0.144	0.021	0.097
S3	0.242	0.268	0.289	0.021	0.18
S4	0.179	0.286	0.214	0.285	0.036
S5	0.092	0.328	0.269	0.017	0.294

Table 2. State transition matrix for weather changes in Tianjin over the past 9 years

State	S1	S2	S3	S4	S5
S1	0.521	0.281	0.122	0.031	0.045
S2	0.31	0.34	0.169	0.039	0.142
S3	0.307	0.269	0.231	0.028	0.165
S4	0.233	0.205	0.13	0.356	0.076
S5	0.199	0.269	0.178	0.009	0.345

Table 3. The stationary state corresponding to the state transition matrix

Data set	Smooth states corresponding to different data sets				
	S1	S2	S3	S4	S5
2021-2023	0.338	0.35	0.178	0.025	0.109
2015-2023	0.368	0.292	0.161	0.045	0.134

From the comparison of the magnitude of the values of the data in Tables 1 and 2, the state transfer matrices derived from the weather data of the last 3 years and the last 9 years are numerically similar, indicating that the changes in the weather of Tianjin in the last 10 years have been smooth in general. From the smooth states corresponding to different weather types in Table 3, the calculated ratio of the smooth state of the S4 (haze) weather type based on the nearly 9 years and nearly 3 years of data is 1.7, which is much more than that of other weather types, which is consistent with the results of the data counted in Figure 3. Combined with the application requirements of PV output modeling, this study used the resultant data shown in Table 1 to carry out a follow-up study.

Modeling the Mean and Fluctuation Values of the No-shade Coefficient of Photovoltaic Output

Let the number of valid PV data in the i-th time window be n. Based on the time series of no-shade coefficient of PV output obtained from Equation (2), and then based on Equation (5), the mean and fluctuation values of no-shade coefficient for that day can be calculated.

$$\begin{cases} \overline{u}_i = \dfrac{\sum_{j=1}^{n} u_{ij}}{n} \\ \Delta U_i = \left\{ u_{ij} - \overline{u}_i \mid j = 1, 2 \cdots n \right\} \end{cases} \tag{5}$$

In Equation (5), u_{ij} is the PV output no-shade coefficient at the j-th moment of the i-th time window, $\overline{u}_i$ is the average value of the no-shade coefficient, and ΔU_i is the fluctuation sequence of the PV output no-shade coefficient.

Due to the diversity of weather, there may be variability in the mean value of the no-shade coefficient for the same weather type, and for different weather types, a statistical plot of the distribution of the mean value of the no-shade coefficient is given in Figure 4. Figure 5 gives a statistical plot of the distribution of the fluctuation of the no-shade coefficient corresponding to Figure 4.

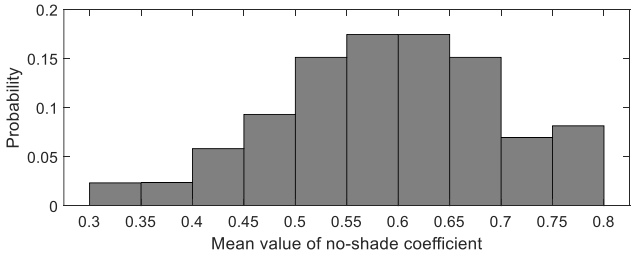

a. sunny

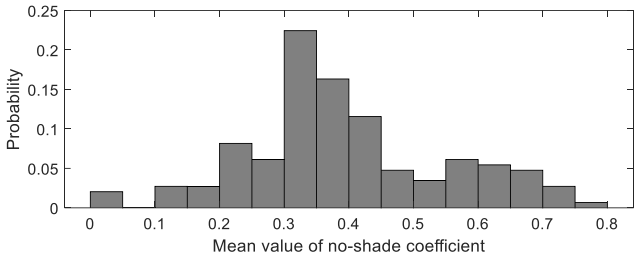

b. cloudy

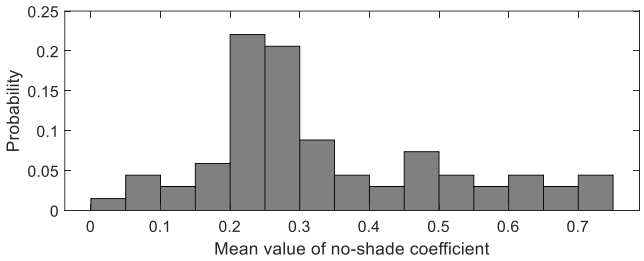

c. overcast sky

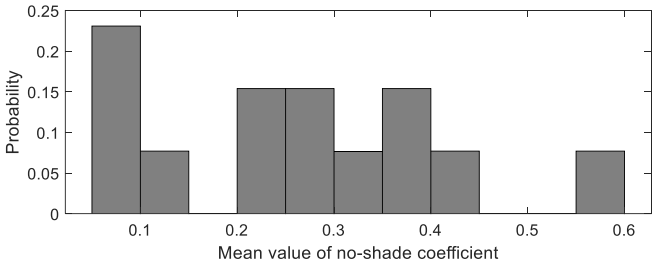

d. haze

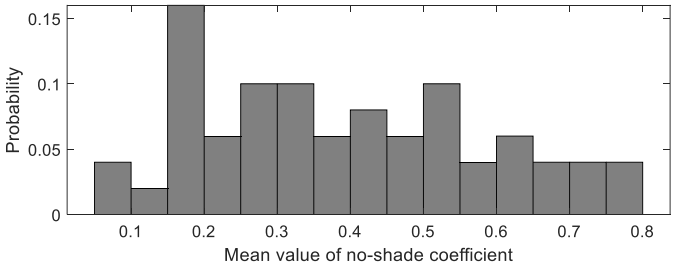

e. rain and snow

Figure 4. Statistics of mean values for the no-shade coefficient across different weather types

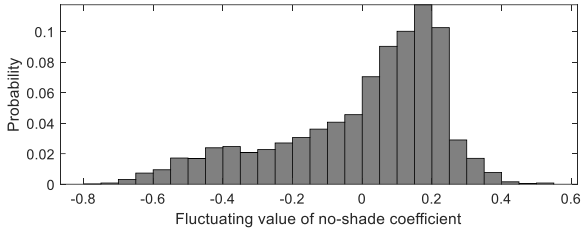

a. sunny

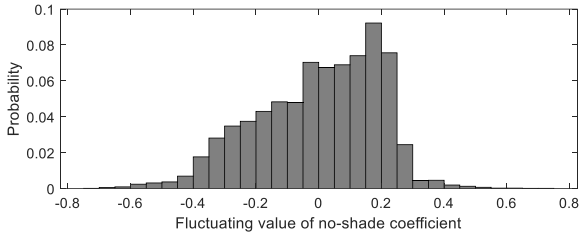

b. cloudy

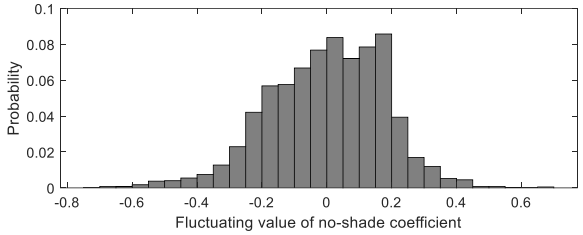

c. overcast sky

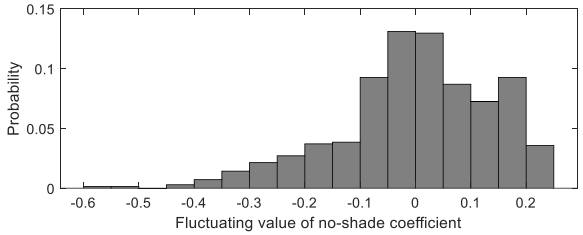

d. haze

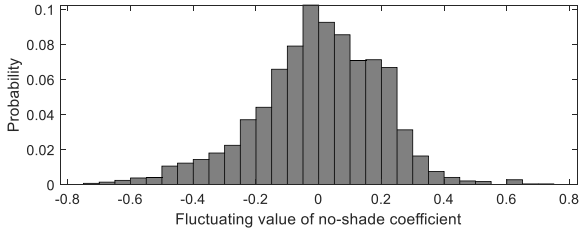

e. rain and snow

Figure 5. Statistics of fluctuation values for the no-shade coefficient across different weather types

In Figure 5, the distribution patterns of the fluctuation values of the no-shade coefficient of different weather types are more homogeneous, which can be described by the normal distribution probability density function shown in Equation (6). While in Figure 4, the distribution of the mean values of the no-shade coefficient of different weather types has a large variability, and its distribution may be characterized by a multi-peak situation, which is more complex and suitable to be fitted by a mixed Gaussian distribution probability density function (Gaussian Mixed Model, GMM) shown in Equation (7) [20].

$$\rho(x) = N(\mu, \sigma) = \frac{1}{\sqrt{2\pi}\sigma} e^{-\frac{(x-\mu)^2}{2\sigma^2}} \tag{6}$$

$$GMM = \sum_{k=1}^{m} \lambda_k N_k(\mu_k, \sigma_k) \tag{7}$$

Equation (6) where x is the random variable, μ and σ are the overall mean and standard deviation of the sample, respectively. Equation (7) where m and k are the total number and index number of Gaussian distribution functions, respectively, and λ is the weight of each function.

In Equation (7) m, λ, μ and σ are the optimization variables and the corresponding computational flow is shown in Figure 6.

When fitting a GMM, it is very important to choose the right number of components, AIC and BIC are commonly used model selection criteria. The core idea of AIC is to prevent overfitting by penalizing many parameters. The smaller the value of AIC, the better the model is. BIC is similar to AIC but it penalizes the model complexity more strongly and BIC tends to select simpler models. Based on the minimum values of AIC and BIC, we can determine the optimal m value.

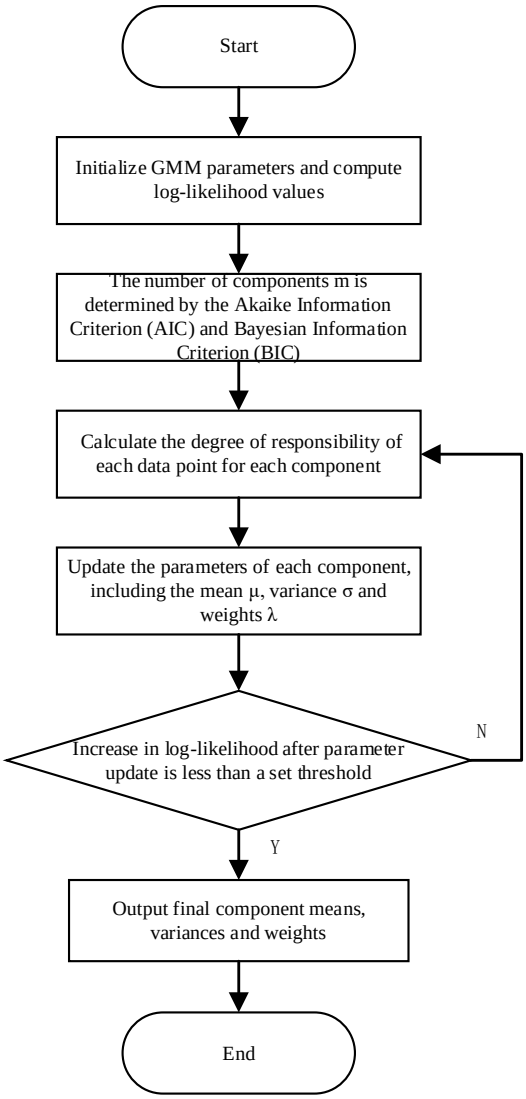

Figure 6. GMM optimization process

Steps in Constructing a PV Time-series Fluctuation Model

The steps of the methodology for modeling PV output volatility based on weather random sampling are summarized as follows:

1. Calculate the no-shade output according to Equation (1), and calculate its corresponding no-shade coefficient according to Equation (2);

2. Analyze the time interval between the PV output time series and the weather time series to determine the width of the time window for analysis and calculation;

3. Construct the Markov chain model of weather type change based on the weather time series and time window;

4. Calculating the mean and fluctuation values of the PV no-shade coefficient according to the time window based on Equation (5);

5. Modeling the mean and fluctuation values of no-shade coefficient based on Equation (6) and Equation (7);

6. Setting an initial weather type S0, S0∈{S1, S2, S3, S4, S5}, and randomly generating a sequence of simulated values of the weather type based on the Markov chain model of step 3;

7. For each sample of the weather type sequence generated in step 6, generating a random number of sequences of no-shade coefficient mean simulated values and fluctuation simulated values based on the no-shade coefficient mean and fluctuation value model of step 5, which are superimposed to synthesize the photovoltaic power generation no-shade coefficient, and thereby generating a photovoltaic power generation simulated power time series based on the no-shade PV output of step 1;

8. Repeating step 7 until all weather simulation sequences are calculated.

EXPERIMENT AND ANALYSIS

The proposed algorithm is validated by taking the operation data of a PV power plant in Wuqing area of Tianjin as an example. In order to fully consider the impact of hazy weather on PV power generation and to obtain a sufficient number of samples, we select the PV operation data in 2021, corresponding to a time interval of 15 minutes. The selected weather type data spans 3 years, from 2021 to 2023, with a time interval of 1 day, where the time window width is taken as 1 day.

Comparison of Simulated and Actual Data for Weather Types

Based on the weather type change state transfer matrix in Table 1, 1-year and 10-year data are generated respectively, and the number of different types of weather is counted, and the corresponding results are shown in Table 4.

Table 4. Comparison of simulated data with actual data for weather types

Data type	Percentage of weather types (%)				
	S1	S2	S3	S4	S5
2021-2023 actual data	32.86	35.52	17.98	2.44	11.2
1 year of simulated data	35.62	35.89	15.62	1.64	11.23
10 year of simulated data	33.42	34.62	18.05	3.12	10.79

As seen in Table 4, along with the increase in simulation duration, the proportion of different types of weather in the simulated data is closer to the actual data, which is consistent with the smooth state corresponding to the 2021-2023 dataset in Table 3.

Volatility Model Parameterization and PV Output Simulation

The PV output volatility model parameters corresponding to this example data are given in Table 5 and Table 6, respectively.

Table 5. Model parameters for the no-shade coefficient mean values

Types of weather	Model parameters			
	Grades m	Weights λ	Average value μ	Standard deviation σ
S1	1	λ=1	μ=0.5914	σ=0.1072
S2	2	λ_1=0.6119 λ_2=0.3881	μ_1=0.3917 μ_2=0.2440	σ_1=0.1954 σ_2=0.0387
S3	3	λ_1=0.4404 λ_2=0.2312 λ_3=0.3284	μ_1=0.3673 μ_2=0.6183 μ_3=0.2705	σ_1=0.0469 σ_2=0.0714 σ_3=0.1105
S4	1	λ=1	μ=0.2614	σ=0.1476
S5	2	λ_1=0.3863 λ_2=0.6137	μ_1=0.2074 μ_2=0.5006	σ_1=0.0775 σ_2=0.1533

Table 6. Model parameters for the no-shade coefficient fluctuation values

Types of weather	Model parameters	
	Average value μ	Standard deviation σ
S1	0	0.2354
S2	0	0.1792
S3	0	0.1952
S4	0	0.1400
S5	0	0.1985

Based on the model parameters 1 year of PV simulated output data is generated as shown in Figure 7. Typical output characteristics for different types of weather simulations are shown in Figure 8.

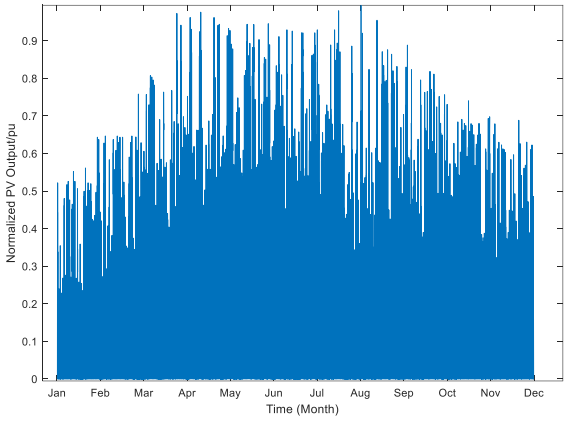

Figure 7. Simulated PV output (1 year)

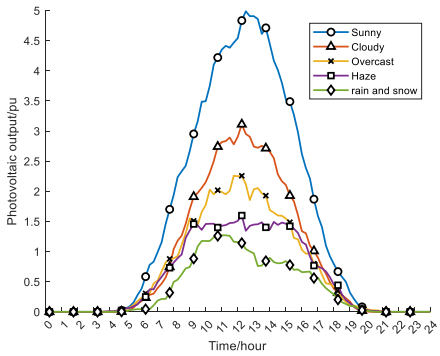

Figure 8. Typical simulated PV output for different weather types

The probability statistics of the simulated and actual PV output, respectively, are described by the β-distribution, and the corresponding probability curves are shown in Figure 9.

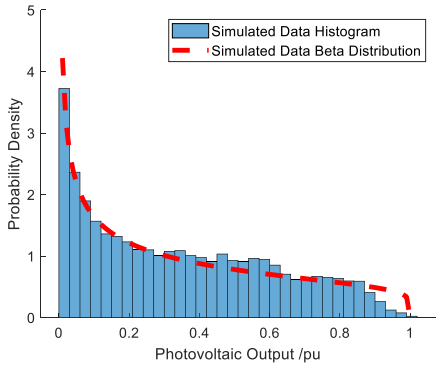

a. Actual PV output

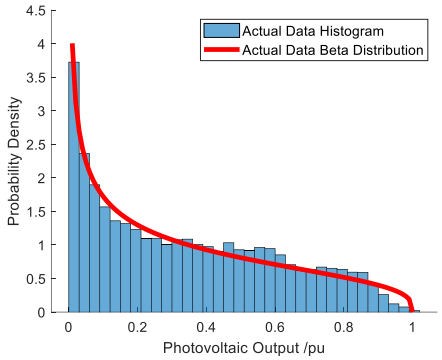

b. Simulated PV output

Figure 9. Comparison of probability distribution between simulated and actual PV output

As can be seen in Figure 9, the probability distribution curves of the PV simulated output and actual output are very close, in which the α parameters corresponding to the β distribution of the actual and simulated outputs are 0.732 and 0.593, respectively, and the β parameters are 1.413 and 1.144, respectively, and the two distribution curves are very close. This verifies the effectiveness of the proposed PV output volatility modeling method.

CONCLUSION

In this paper, a PV output volatility modeling method is proposed through in-depth study of the impact of weather stochasticity on PV output volatility. The method integrates the Markov chain weather type model with the mean and fluctuation value model of the no-shade coefficient, which not only takes into account the stochastic characteristics of the weather type conversion, but also finely portrays the fluctuation characteristics of the PV output under different weather conditions.

In addition, the study in this paper reveals the intrinsic connection between weather type and PV output volatility, which provides a new perspective to deeply understand the stochasticity and uncertainty of PV output. The proposed model and methodology are not only applicable to the modeling of PV output volatility, but also can provide reference for the forecasting and volatility analysis of other new energy sources, such as wind energy and hydroelectric energy.

In the future, on the basis of wider and finer data, we will further explore the impact of more complex weather changes, and carry out model parameter sensitivity analyses in combination with PV operation and maintenance status and equipment aging degree to enhance the applicability and generalization ability of the model.

ACKNOWLEDGMENTS

This work was supported by the project "(Chengxi-R&D 2023-01) Research on Distributed Photovoltaic Operation Risk Perception and Model-free Adaptive Regulation Technology for Distribution Network" of State Grid Tianjin Electric Power Company in China.

REFERENCES

[1] Li, R., Hu, Y., Wang, X., et al. "Estimating the impacts of a new power system on electricity prices under dual carbon targets." Journal of Cleaner Production 438 (2024): 140583.
[2] Zhou, S., Li, Y., Jiang, C., et al. "Enhancing the resilience of the power system to accommodate the construction of the new power system: Key technologies and challenges." Frontiers in Energy Research 11 (2023): 1256850.
[3] Hao, W., Xiao, W., Yan, Q., et al. "Evaluation of distributed photovoltaic economic access capacity in distribution networks considering proper photovoltaic power curtailment." Energies 17.17 (2024): 4441.
[4] Feron, S., Cordero, R. R., Damiani, A., et al. "Climate change extremes and photovoltaic power output." Nature Sustainability 4.3 (2021): 270-276.
[5] Qiu, Y., Guo, X., Wang, Y., et al. "Prediction of photovoltaic modules output performance and analysis of influencing factors based on a new optical-electrical-thermal-fluid coupling model." Energy Conversion and Management 321 (2024): 119051.
[6] Kumar, N., Hussain, I., Singh, B., et al. "Rapid MPPT for uniformly and partial shaded PV system by using JayaDE algorithm in highly fluctuating atmospheric conditions." IEEE Transactions on Industrial Informatics 13.5 (2017): 2406-2416.
[7] Jun, D., Chen, Z., and Dou, X. "The influence of multiple types of flexible resources on the flexibility of power system in northwest China." Sustainability 14.18 (2022): 11617.
[8] Maitanova, N., Schlüters, S., Hanke, B., et al. "Quantifying power and energy fluctuations of photovoltaic systems." Energy Science & Engineering 10.12 (2022): 4496-4511.
[9] Khelifi, R., Guermoui, M., Rabehi, A., et al. "Short-term PV power forecasting using a hybrid TVF-EMD-ELM strategy." International Transactions on Electrical Energy Systems 2023.1 (2023): 6413716.
[10] Gupta, P., and Singh, R. "Effect of PV power forecast error on the frequency of a standalone microgrid system." Journal of Renewable and Sustainable Energy 16.4 (2024).
[11] Putra, J. T., and Setyonegoro, M. I. B. "Modeling of high uncertainty photovoltaic generation in quasi dynamic power flow on distribution systems: A case study in Java Island, Indonesia." Results in Engineering 21 (2024): 101747.
[12] Ai, Q., Xiang, J., Liu, Y., et al. "Multi-scenario flexibility assessment of power systems considering renewable energy output uncertainty." Frontiers in Energy Research 12 (2024): 1359233.
[13] Wang, J., Yu, Y., Zeng, B., et al. "Hybrid ultra-short-term PV power forecasting system for deterministic forecasting and uncertainty analysis." Energy 288 (2024): 129898.
[14] Venkateswari, R., and Sreejith, S. "Factors influencing the efficiency of photovoltaic system." Renewable and Sustainable Energy Reviews 101 (2019): 376-394.
[15] Jordan, Dirk C., Perry, K., White, R., et al. "Extreme weather and PV performance." IEEE Journal of Photovoltaics (2023).
[16] Lim, J. H., Lee, Y. S., and Seong, Y. B. "Diurnal thermal behavior of photovoltaic panel with phase change materials under different weather conditions." Energies 10.12 (2017): 1983.
[17] Cui, S., Lyu, S., Ma, Y., et al. "Improved informer PV power short-term prediction model based on weather typing and AHA-VMD-MPE." Energy 307 (2024): 132766.
[18] Yi, D., Yu, M., Wang, Q., et al. "Method for Wind–Solar–Load extreme scenario generation based on an improved InfoGAN." Applied Sciences 14.20 (2024): 9163.
[19] Eker, Sibel. "Drivers of photovoltaic uncertainty." Nature Climate Change 11.3 (2021): 184-185.
[20] Collas, A., Breloy, A., Ren, C., et al. "Riemannian optimization for non-centered mixture of scaled Gaussian distributions." IEEE Transactions on Signal Processing (2023).